IOPscience iopscience.iop.org

Home Search Collections Journals About Contact us My IOPscience

The local atomic quasicrystal structure of the icosahedral $Mg_{25}Y_{11}Zn_{64}$ alloy

This article has been downloaded from IOPscience. Please scroll down to see the full text article.

2005 J. Phys.: Condens. Matter 17 1561

(http://iopscience.iop.org/0953-8984/17/10/011)

View the table of contents for this issue, or go to the journal homepage for more

Download details:
IP Address: 129.252.86.83
The article was downloaded on 27/05/2010 at 20:25

Please note that terms and conditions apply.

INSTITUTE OF PHYSICS PUBLISHING JOURNAL OF PHYSICS: CONDENSED MATTER

J. Phys.: Condens. Matter **17** (2005) 1561–1572 doi:10.1088/0953-8984/17/10/011

The local atomic quasicrystal structure of the icosahedral $Mg_{25}Y_{11}Zn_{64}$ alloy

S Brühne[1], E Uhrig[1], C Gross[1], W Assmus[1], A S Masadeh[2] and S J L Billinge[2]

[1] Physikalisches Institut, Johann Wolfgang Goethe-Universität, Robert-Mayer-Straße 2-4, D-60054 Frankfurt/Main, Germany
[2] Department of Physics and Astronomy and Center for Fundamental Materials Research, Michigan State University, East Lansing, MI 48824-1116, USA

Received 21 October 2004, in final form 3 February 2005
Published 25 February 2005
Online at stacks.iop.org/JPhysCM/17/1561

Abstract

A local and medium range atomic structure model for the face centred icosahedral (fci) $Mg_{25}Y_{11}Zn_{64}$ alloy has been established in a sphere of $r = 27$ Å. The model was refined by least squares techniques using the atomic pair distribution (PDF) function obtained from synchrotron powder diffraction. Three hierarchies of the atomic arrangement can be found: (i) five types of local coordination polyhedra for the single atoms, four of which are of Frank–Kasper type. In turn, they (ii) form a three-shell (Bergman) cluster containing 104 atoms, which is condensed sharing its outer shell with its neighbouring clusters, and (iii) a cluster connecting scheme corresponding to a three-dimensional tiling leaving space for a few glue atoms. Inside adjacent clusters, Y_8 cubes are tilted with respect to each other and thus allow for overall icosahedral symmetry. It is shown that the title compound is essentially isomorphic to its holmium analogue. Therefore, fci-Mg–Y–Zn can be seen as the representative structure type for the other rare earth analogues fci-Mg–Zn–RE (RE = Dy, Er, Ho, Tb) reported in the literature.

(Some figures in this article are in colour only in the electronic version)

1. Introduction

Since the discovery of icosahedral Al–Mn in 1984 [1] the determination of the atomic-scale structure of quasicrystals remains a difficult problem [2]. Another class of metastable icosahedral alloys is Mg–Zn based, containing Al or Ga. In 1993, Luo *et al* [3] discovered stable ternary Mg–Y–Zn quasicrystals with icosahedral diffraction symmetry. Y can also be substituted by Dy, Er, Gd, Ho and Tb [4]. Since 1998, single crystals have been available for Mg–Zn–RE (RE = Dy, Er, Ho, Tb) [5, 6]. The crystals exhibit a six-dimensional lattice parameter $a(6D) \approx 2 \times 5.2$ Å and an F-type centring called face-centred icosahedral (fci).

 © 2005 IOP Publishing Ltd Printed in the UK

Fci-Mg–Y–Zn shows virtually no diffuse scattering and therefore is considered to be of high structural perfection [7]. Mg–Zn–RE quasicrystals of comparable quality but with a P-type lattice, $a(6D) \approx 5.2$ Å are also known [8]. They are called simple icosahedral (si) and are found at higher zinc–magnesium ratios for RE = Er, Ho and Tm [9, 10].

To date, the following structure analyses of icosahedral Mg–Zn–RE quasicrystals are available: fci-Ho–Mg–Zn was refined in 6D and the derived 3D physical space information is given on the Ho partial structure in the twofold plane [11]. Information on atomic clusters in fci-Mg–Tb–Zn was obtained from HRTEM and x-rays in [12] and a 6D Rietveld refinement of x-ray powder data revealed the average decoration of 3D Penrose tiles for fci-Ho–Mg–Zn [13]. Another 3D model for fci-Mg–Y–Zn was obtained by Fourier transform of single x-ray diffraction data [14]. In 2003 a quantitative analysis of the atomic pair distribution function (PDF) of si-Ho–Mg–Zn from in-house x-ray powder diffraction was performed and resulted in the element distribution and geometry of a 105-atom Bergman cluster [15]. The approach was based on rational approximant models for the local quasicrystal structure: while the 3D quasiperiodic structure can be generated from 6D via an irrational projection (using $\tau = (\sqrt{5}+1)/2$ in the projection matrix), a periodic p/q approximant is generated using p/q instead of τ. As the PDF always reflects the *local* structure, the short range structure of the quasicrystal was refined *as if* it was a $1/1$-approximant in a sphere confined to $r < 17$ Å [15]. A larger $2/1$-approximant model contains eight such clusters and was similarly refined, in better agreement with the data, for fci-Ho–Mg–Zn with $r < 27$ Å [16]. Thus the PDF approach represents a complementary technique which has just recently yielded detailed insight into the atomic structure of icosahedral Mg–Zn–RE phases.

In [16] we discussed the idea of 'virtual' rational p/q-approximant models for the local structure of fci-Ho–Mg–Zn in detail. A cubic $2/1$-approximant unit cell ($a \approx 23$ Å and symmetry restrictions *as if* in $Pa\bar{3}$ [18]) can serve as a coordinate system for the local model. In the present paper, that model has been adapted for the fci-Mg–Y–Zn phase. We use high Q_{max} synchrotron powder diffraction data to generate a well resolved PDF for least-squares structure refinements. The questions to answer are 'Can synchrotron data confirm our earlier results [16] from in-house x-rays?' and 'Is the Y compound isostructural to the Ho compound?'. If yes, this would open a perspective for future use of difference PDFs since the PDF is a function on an absolute scale. Thus *local* atomic models containing only the RE positions, i.e. only ∼10% of all constituting atoms, could be used: regarding the high unit cell contents (160, 680, 2888 or ∼12 200 atoms for $1/1$, $2/1$, $3/2$ or $5/3$ models, respectively [15]), this option would clearly simplify future structure calculations which are needed to understand the *quasiperiodic* structure.

2. Experimental details

2.1. Synthesis and basic characterization

Single-crystalline material of fci-Mg–Y–Zn has been obtained from the melt using the liquid-encapsulated top-seeded solution growth method (LETSSG) as described in [5]. Laue diffractograms of the grains exhibit symmetry $m\bar{3}\bar{5}$. The composition was determined to be 64 at.% Zn, 25 at.% Mg and 11 at.% Y by wavelength dispersive analysis of x-rays (WDX; Microspec WDX3PC) of polished samples within an accuracy of ±1 at.% versus standard specimens of the pure metals. Thus the formula for the title compound was chosen as $Mg_{25}Y_{11}Zn_{64}$. Its density was determined to be $\rho = 5.0(1)$ g cm^{-3} measured by a He pycnometer Micrometrics AccuPyc 1330. The x-ray powder diffractogram (Siemens Kristalloflex 810, Cu Kα, $\lambda = 1.541$ Å) could be indexed with an F-centred lattice parameter

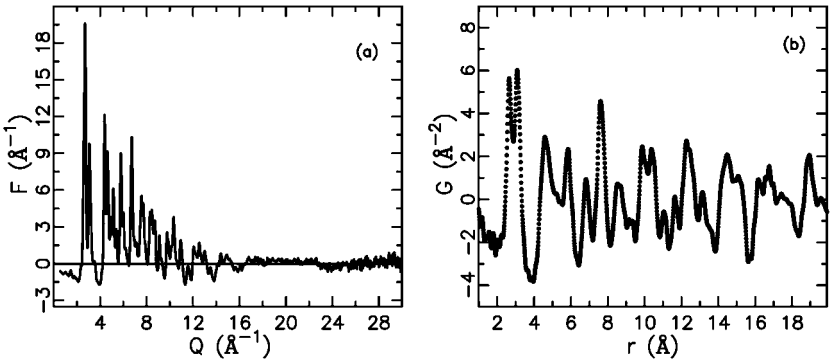

Figure 1. (a) The experimental reduced structure function $F(Q) = Q[S(Q) - 1]$ of fci-$Mg_{25}Y_{11}Zn_{64}$ with Q_{max} cut at 30.0 Å^{-1} and (b) the corresponding PDF, $G(r)$.

a(6D) $\approx 2 \times 5.19(2)$ Å (reflection condition $h_1h_2h_3h_4h_5h_6$: h_i all even or all odd) using Elser's method [9, 19].

2.2. Data collection

The real-space pair distribution function (PDF), $G(r)$, gives the probability of finding pairs of atoms separated by distance r, and comprises peaks corresponding to all discrete interatomic distances. The experimental PDF is a direct Fourier transform of the total scattering structure function $S(Q)$, the corrected, normalized intensity, from powder scattering data given by

$$G(r) = \frac{2}{\pi}\int_0^\infty Q[S(Q) - 1]\sin Qr\,\mathrm{d}Q,$$

where $Q = \frac{4\pi}{\lambda}\sin\theta$ is the magnitude of the scattering vector. Unlike crystallographic techniques, the PDF incorporates both Bragg and diffuse scattering intensities, resulting in local structural information [17, 20]. Its high real-space resolution is ensured by measurement of scattering intensities over an extended Q range $Q_{max} \geqslant 35.0$ Å^{-1} using short wavelength x-rays or neutrons.

The diffraction experiment was performed on a powdered sample at the 6ID-D μCAT beamline at the Advanced Photon Source (APS) at Argonne National Laboratory. Data acquisition at 300 K employed the recently developed rapid acquisition PDF (RA-PDF) technique [21] with an x-ray energy of 130.0 keV. Data were collected using an image plate camera (Mar345), with a usable diameter of 345 mm, mounted orthogonal to the beam path with sample to detector distance of 220 mm. Lead shielding before the goniometer, with a small opening for the incident beam, was used to reduce the background. All raw data were integrated using the software Fit2D [22] and converted to intensity versus 2θ (the angle between incident and the scattered x-rays). The integrated data were normalized with respect to the average monitor count, then transferred to the program PDFgetX2 [23] to carry out data reduction to obtain $S(Q)$ and the PDF $G(r)$ which are shown in figure 1.

2.3. Structure refinements

For the least squares structure refinement the program PDFFIT [24] was used. The starting model has the atomic coordinates of the '2/1' model for the local structure of fci-Ho–Mg–Zn [16] where Ho was replaced by Y. The cubic lattice parameter was set to $a = 23.0$ Å and

Table 1. Data for the final least squares refinements of the local atomic structure of fci-$Mg_{25}Y_{11}Zn_{64}$ as if it were its cubic 2/1 approximant.

Scale factor	1.562(3)
Dynamic correlation factor δ (Å^3)	0.5159(2)
Low r/σ ratio	1.0
Virtual approximant space group [18]	$Pa\bar{3}$ (no. 205)
Virtual approximant lattice parameter a(3D) (Å)	23.0291(5)
Calculated hypercubic lattice parameter a(6D) (Å)	2×5.170
Refinement r range (Å)	2–27
Number of data points used	832
λ (Å^{-1})	0.095
Termination at Q_{max} (Å^{-1})	30.0
Calculated model composition	$Mg_{21.2}Y_{10.6}Zn_{68.2}$
Calculated model density ρ (g cm^{-3})	5.436
Q resolution $\sigma(Q)$ (Å^{-1})	0.017
Number of refined parameters	120
R-value	0.1371

all temperature factors were set to $U_{eq} = 1.5 \times 10^{-2}$ Å^{-2} for the beginning. The 832 data points in the r-range 2–27 Å were used for the refinements. This is a range of approximately 1.2 times the 'virtual' lattice constant. Symmetry restrictions of $Pa\bar{3}$ [18] were retained for the atomic coordinates since this space group describes properly the 'real' 2/1 approximants e.g. in the Al–Mg–Zn system. In a first step the scale factor, the dynamic correlation factor δ and lattice constant a were refined. Then the temperature factors U_{eq} were allowed to relax and finally the positional parameters xyz were included in the refinements. Since U_{eq} of Mg5 (nomenclature as in [16]) dropped to less than 0.01×10^{-2} Å^{-2}, it was replaced by a zinc atom (Zn21). The refinements converge finally at $R = 13.7\%$. The final plot of observed, calculated and difference data is given in figure 2(a); the difference plot is almost featureless. U_{eq} scatter statistically (see table 2)—they 'bury' the limitedness of the periodic model for an aperiodic structure. There is one exception (Y3) that is discussed in sections 3.2 and 3.3. The resulting data were analysed with respect to crystal-chemical validity [25]. Data concerning the refinement are listed in table 1. Figure 2(b) compares the quasicrystal x-ray powder pattern to a simulated diffractogram of the 2/1-approximant model (data from table 2). The simulation clearly reproduces the character of the experimental intensity distribution. Of course, the local model cannot match the positions of the reflections which are governed by long-range periodicity or quasiperiodicity, respectively.

3. Results and discussion

The structure refinements result in a data set for the local model for fci-$Mg_{25}Y_{11}Zn_{64}$, which is listed in table 2. The data give rise to a structure description in terms of structural hierarchies. This will be discussed in sections 3.1 and 3.2. The section 3.3 contains a comparison to fci-$Ho_9Mg_{26}Zn_{65}$.

3.1. Structure description

Three structural hierachies are observed on different length scales in fci-Mg–Y–Zn:

(i) Local atomic coordination polyhedra ($r < 4$ Å) all exhibit coordination numbers (CN) 11, 12, 14, 15 or 16 with the same topologies, respectively.

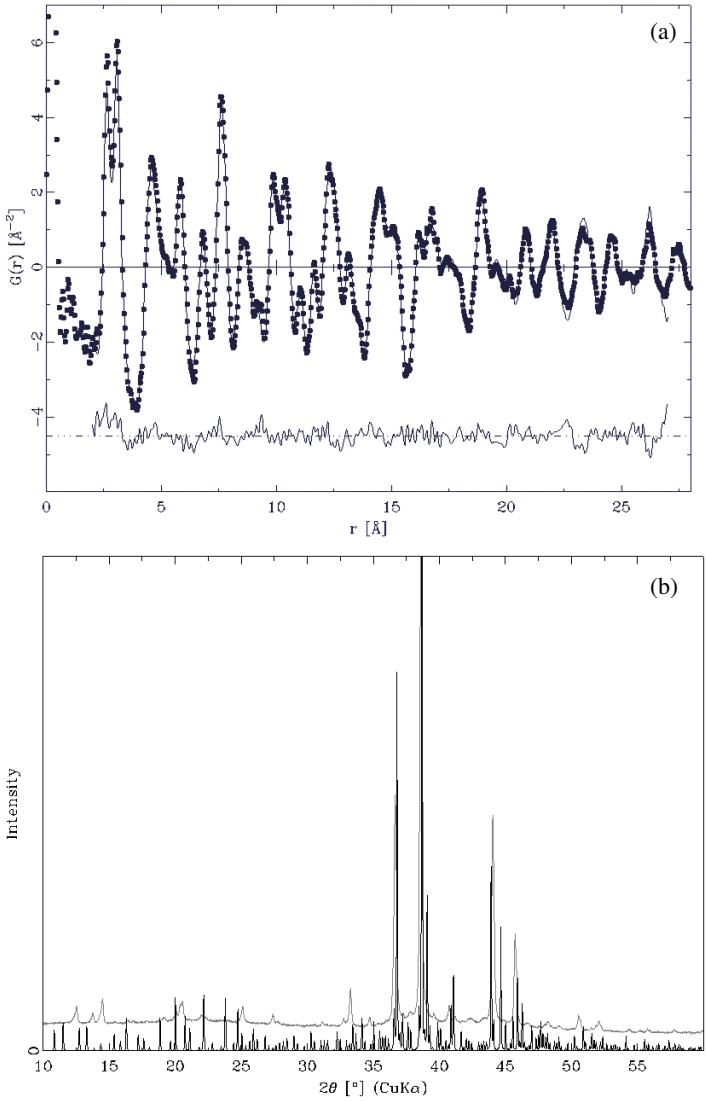

Figure 2. (a) Local model in direct space: PDF $G(r)$ from synchrotron data of fci-$Mg_{25}Y_{11}Zn_{64}$ (dots), PDF calculated for the local atomic structure as if it were its cubic 2/1 approximant (r_{max} = 27 Å, solid curve) and their difference plot below (R = 13.7%). (b) Reciprocal space: x-ray powder diffractogram of fci-$Mg_{25}Y_{11}Zn_{64}$ (grey line) compared to a simulated diffractogram of the 2/1-approximant model (black curve). Note that the intensity distribution of the reflections is roughly reproduced.

(ii) The atoms of (i) group to units of 104 atoms (Bergman cluster, $r \approx 15$ Å).
(iii) These clusters are arranged on the vertices of a canonical cell tiling (CCT, [29]). There are only two tiling edge lengths: ∼12 and ∼14 Å.

Note that due to the self-similar character of quasicrystalline structures the icosahedral topology will be observed at different points: as local coordination polyhedra (CN 12, to be found all over the structure), in shell 1 and 2b of the cluster and finally as overall diffraction symmetry. The three structural hierarchies (i)–(iii) will be addressed below:

Table 2. Structural data of fci-$Mg_{25}Y_{11}Zn_{64}$: the quasicrystal is described locally as if it were a 2/1-approximant, $a = 23.0291(5)$ Å with symmetry restrictions of space group $Pa\bar{3}$ (no. 205 [18]). The atom numbering scheme corresponds to [16] for reasons of comparability. The average interatomic distance $\langle d \rangle$ is given for the first coordination shell with coordination number CN. Values in **bold** are discussed in the text.

Atom type	Atom no.	Wyckoff position *as if* in $Pa\bar{3}$	x/a	y/a	z/a	U_{eq} (10^{-2} Å^2)	CN	$\langle d \rangle$ (Å)
α^0	[void]	8c	0.3458	x	x	[-]	12	2.581
α^1	Zn16	24d	0.253 42(16)	0.291 18(15)	0.351 61(12)	0.540(19)	11	2.829
	Zn17	24d	0.254 91(13)	0.409 82(15)	0.344 95(19)	0.804(21)	11	2.838
	Zn18	24d	0.288 99(15)	0.346 36(21)	0.447 22(14)	1.067(23)	11	2.864
	Zn19	24d	0.345 29(15)	0.440 84(13)	0.406 54(19)	0.619(15)	11	2.979
α^2	Zn1	24d	0.027 05(23)	0.471 24(25)	0.164 39(25)	1.53(4)	12	3.068
	Zn3	24d	0.040 946(6)	0.230 18(11)	0.159 087(5)	0.3962(3)	12	2.935
	Zn14	24d	0.155 81(23)	0.238 6(24)	0.356 91(22)	1.59(4)	12	2.882
	Zn15	24d	0.162 9(3)	0.464 2(4)	0.356 89(20)	2.52(5)	12	2.889
α^3	Zn2	24d	0.044 38(18)	0.131 40(17)	0.101 26(20)	1.10(3)	12	3.007
	Zn6	24d	0.052 26(19)	0.289 62(22)	0.340 63(23)	1.27(3)	12	2.924
	Zn7	24d	0.073 0(3)	0.091 1(3)	0.497 4(3)	1.72(6)	12	3.056
	Zn8	24d	0.068 79(23)	0.391 40(21)	0.352 57(22)	1.31(4)	12	2.862
	Zn9	24d	0.094 67(18)	0.467 35(23)	0.445 68(19)	0.90(3)	12	2.919
	Zn10	24d	0.095 0(3)	0.469 9(3)	0.253 1(3)	1.38(4)	12	3.053
	Zn11	24d	0.101 37(17)	0.230 30(18)	0.256 41(20)	0.654(21)	12	2.860
	Zn12	24d	0.139 35(19)	0.404 43(21)	0.163 17(21)	0.97(3)	12	3.020
	Zn13	24d	0.133 25(15)	0.288 73(19)	0.156 76(21)	0.937(22)	12	2.858
β	Mg3	24d	0.053 6(6)	0.305 0(6)	0.066 6(5)	1.03(9)	16	3.352
	Mg7	24d	0.162 2(4)	0.332 6(4)	0.277 5(4)	0.59(5)	16	3.184
	Mg8	24d	0.226 10(9)	0.257 816(5)	0.466 562(6)	0.2783(3)	16	3.206
	Mg9	24d	0.213 2(11)	0.471 8(10)	0.439 7(11)	3.71(21)	16	3.242
	Y1	24d	0.036 81(12)	0.350 47(15)	0.224 57(15)	0.632(15)	16	3.137
	Y2	24d	0.149 57(21)	0.349 1(3)	0.422 1(3)	2.04(4)	16	3.155
	Y3	8c	0.235 6(17)	x	x	**25.0(9)**	16	3.130
	Y4	8c	0.460 85(17)	x	x	1.32(5)	16	3.324
γ	Zn5	24d	0.056 0(3)	0.133 6(3)	0.237 3(3)	1.80(6)	14	3.010
	Zn21	24d	0.099 2(5)	0.214 2(5)	0.455 3(4)	4.41(13)	14	3.124
δ^X	Mg1	24d	0.033 2(7)	0.354 4(5)	0.462 0(7)	1.56(9)	15	3.131
	Mg4	24d	0.049 9(6)	0.158 4(7)	0.358 0(6)	2.29(12)	15	3.064
δ^Y	Y5	8c	0.158 06(9)	x	x	0.336(21)	16	3.071
δ^Z	Zn20	8c	0.022 0(3)	x	x	1.01(6)	**12**	2.957

ad (i). Except CN 11, the coordination shells are all triangulated and they topologically represent regular, or sometimes distorted, Frank–Kasper polyhedra [26, 27]. According to their metallic radii [28], Zn atoms reside in CN 11, 12 and 14; Mg atoms in CN 15 or 16; all Y atoms require CN 16. Most frequent is the icosahedron (CN 12) for 47% of all atoms. CN 11, however, can be described as CN $(12 - 1)$ since it is topologically an icosahedron that lacks one vertex. For typical examples of the five types of polyhedra, see figure 3.

ad (ii). To define the structural function of the single atoms at the second hierarchical level, they are labelled after [30] using Greek letters: α^1, α^2, α^3, β, γ and δ. Figure 4 explains the architecture of the cluster. It is built of three concentric shells.

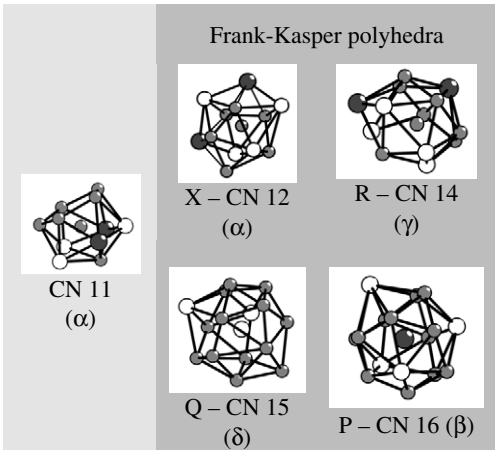

Figure 3. Five types of local coordination polyhedra in fci-Mg–Y–Zn. White balls, Mg atoms; grey, Zn; dark grey, Y. Capital letters denote Frank–Kasper polyhedra [26]; CN: coordination number (Greek letters refer to the structural function of the central atom on the next hierarchy level).

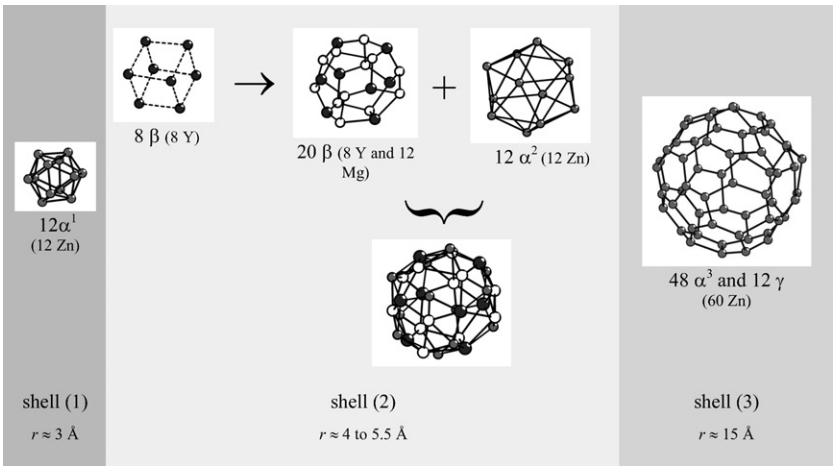

Figure 4. Three concentric shells together build the basic, onion-like structural unit in fci-$Mg_{25}Y_{11}Zn_{64}$ (Bergman cluster, in total 104 atoms). White balls, Mg atoms; grey, Zn; dark grey, Y. First and third shells consist of Zn atoms only; shell (2) shows a distinct distribution of Y, Mg and Zn; eight Y atoms are arranged on the vertices of a cube.

(1) 12 Zn atoms (α^1) are placed around the void cluster centre (α^0) forming an empty icosahedron of $r \approx 3$ Å.

(2a) 12 Mg and 8 Y atoms (β) form a pentagon–dodecahedron. Its ideal (topological) symmetry $m\bar{3}\bar{5}$ is lowered to $m\bar{3}$ since the eight Y atoms form an inscribed cube of edge length 5.4 Å.

(2b) The second shell is completed by 12 Zn atoms (α^2) which lay on the vertices of a τ-inflated analogue of the first shell (icosahedron).

All atoms of shell (2) represent a rhombic dodecahedron of $r \approx 4$ to 5.5 Å.

(3) The third shell consists of $48\alpha^3$ atoms and 12γ atoms, in total 60 Zn atoms arranged like a truncated icosahedron or soccer ball of $r \approx 15$ Å.

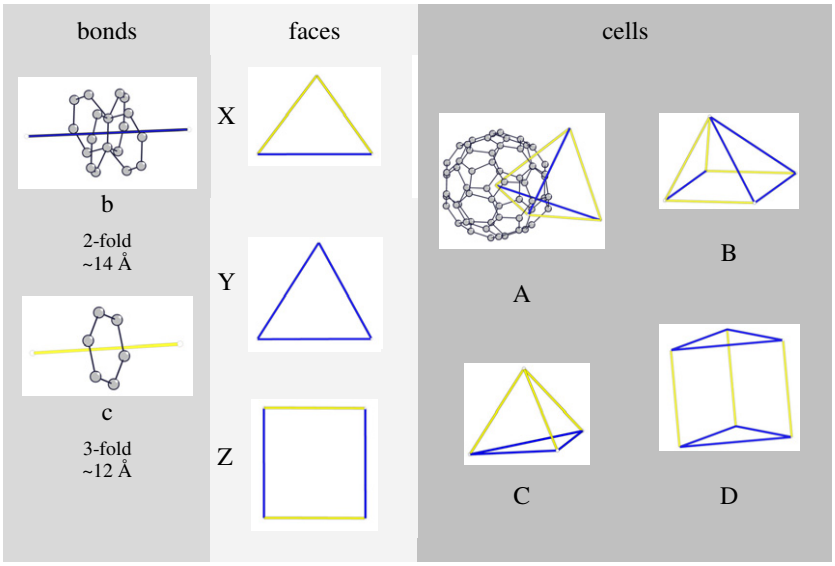

Figure 5. Bonds, faces and cells of the canonical cell tiling (CCT [29]). b-bonds (c-bonds) connect icosahedral objects along their twofold (threefold) symmetry directions. $|c| = (\sqrt{3})/2 \times |b|$. Some atoms of the third shell are drawn in to illuminate the context.

While the innermost shell (1) is an empty regular icosahedron, the outer shells are more distorted due to interaction with neighbouring clusters; see (iii).

ad (iii). The α^3 atoms are shared with the neighbouring clusters and define a so-called 'c-bond' of the CCT. γ atoms are shared as well and define a 'b-bond' of the CCT. The CCT consists of four types of 3D cells (namely A, B, C and D) made of three faces (termed X, Y and Z) which all consist of b- and c-bonds; see figure 5.

In our local 2/1-model each node of the CCT represents a cluster centre. At each node six b-bonds and seven c-bonds meet in such a way that nine A-, three B- and three C-cells fill the whole space around the node as shown in figure 6. This node environment represents the local matching rule for the local model.

In between the clusters, space is filled by so-called glue atoms (δ). Their location is always in the plane of a CCT face, so δ^{X}, δ^{Y} and δ^{Z} atoms are distinguished (see table 2). Both the common α^3 and γ atoms in the third shells and the stuffing with δ atoms implies a close packed structure. Therefore, the term 'cluster' as it is used here must not be mistaken for isolated clusters; see also [2].

3.2. Details of the local model for fci-Mg–Y–Zn

The crystal-chemical validity of the proposed model can be considered by plotting the average distances of central atoms to their coordinating ligands, $\langle d \rangle$. A plot of $\langle d \rangle$ versus coordination number CN is shown in figure 7. The values make chemical sense for the metallic radii present in the structure [28]. There is also a clear trend of increasing $\langle d \rangle$ at higher CN as expected. The excellent agreement of the model with the measured PDF (figure 2(a)) also indicates that the model yields the correct real-space local structure. The outlier at ($\langle d \rangle = 2.581$ Å, CN $= 12$) corresponds to the void at the cluster centre. There is not enough space to accommodate a hypothetical Zn atom which is consistent with this site being a vacancy.

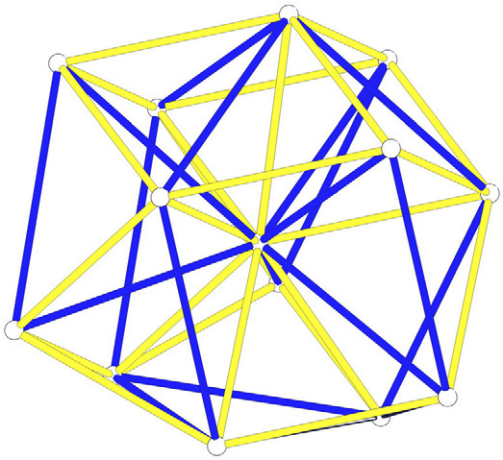

Figure 6. CCT node environment (local matching rule) for the 2/1 approximant local structure model for fci-$Mg_{25}Y_{11}Zn_{64}$.

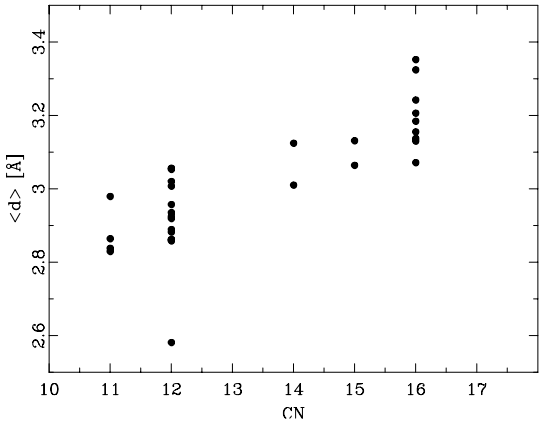

Figure 7. Plot of average interatomic distances $\langle d \rangle$ versus coordination number CN in the local model for fci-Mg–Y–Zn.

There is one unphysically short interatomic distance in the model: d(Zn20–Zn20) = 1.76 Å. Zn20 is a δ^Z glue atom that lies in the rectangular Z face of the CCT. Counting the short distance, the CN would be 13. Instead we can regard it as a split position. A regular CN 12 polyhedron results and the anomalously short Zn–Zn interaction is removed. For this reason we choose the latter scenario and the coordination presented in table 2 reflects this.

The calculated model composition is $Mg_{21.2}Y_{10.6}Zn_{68.2}$. This is somewhat richer in zinc than the measured composition $Mg_{25}Y_{11}Zn_{64}$. The calculated density $\rho_{calc} = 5.436$ g cm^{-3} compares to the measured value $\rho_{meas} = 5.0(1)$ g cm^{-3}. These observations can be accounted for if we assume that some Mg sits on the γ positions, there is a lower occupancy of δ^Z (Zn20) and the measured density is an underestimation of the fully dense material due to the possible presence of pores in the sample. For example, the assumption all γ positions being totally occupied by Mg would lead to $\rho_{calc} = 5.129$ g cm^{-3}.

The Y partial structure consists of Y_8-cubes (Y1 to Y4) of edge length 5.4 Å which are tilted with respect to each other in four of the five different possible orientations to inscribe a

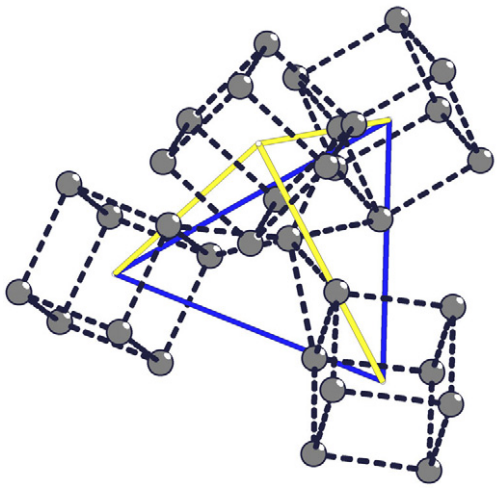

Figure 8. Y partial structure in fci-$Mg_{25}Y_{11}Zn_{64}$ around the four nodes of a canonical C cell. The Y_8 cubes are connected via a central δ^Y glue Y atom. Dotted interatomic spacings Y–Y: 5.4 Å.

cube in a pentagon dodecahedron. In that way global icosahedral symmetry can be achieved in the quasicrystal. Figure 8 explains the interconnection of the cubes *via* the δ^Y glue atom, Y5, attached to a canonical C cell. Here equilateral Y_3-triangles with an edge length of again 5.4 Å occur in a twisted manner around Y5. In [16] steric reasons are brought forward as an argument for the absence of direct RE–RE contacts <5 Å. This is also consistent with findings from an EXAFS investigation [31] and may explain the high temperature factor $U_{eq}(Y3) = 0.25$ Å^2 (see table 2) since Y3 is connected to Y5 at $d = 3.1$ Å in our model.

The details discussed concerning composition, density and especially the properties of Zn20 and Y5 all touch the question for the 'true' cluster connection scheme in the quasicrystal. Beyond the local model developed here, there is evidence for an interpenetration of some of the clusters in higher approximant structures (e.g. 3/2-2/1-2/1-Ga–Mg–Zn, [30]) or other models for fci-Mg–Zn–RE [32, 14]. Unfortunately, an icosahedral quasiperiodic CCT has not been found by mathematicians yet [33]. As is the case for other tiling approaches, there is an intrinsic interdependence between the atomic decoration and the tiles themselves [32]. PDF quasicrystal analysis using an r-range and a model both confined to ∼25 Å cannot give a satisfactory answer to that question.

3.3. Relation to fci-Ho–Mg–Zn

The diffraction patterns of fci-Mg–Y–Zn and fci-Ho–Mg–Zn are very similar. Differences in the intensity distribution hitherto were assumed to be due to the different scattering powers of ^{39}Y and ^{67}Ho. Now we can confirm that the short-range atomic structure of fci-$Mg_{25}Y_{11}Zn_{64}$ is basically identical to that of fci-$Ho_9Mg_{26}Zn_{65}$ [16], both referred to as fci-Mg–Zn–RE (RE = Y; Ho). Compared to our earlier study on the Ho compound we find the following comparisons:

Displacements of the fractional atomic coordinates with respect to a(3D) of the cubic 2/1 model cells are 0.01 on average and 0.04 at maximum; this means 0.3 and 0.9 Å, respectively, on an absolute scale. The cluster centres (α^0) in both phases are not occupied and the α^1 atoms

form a regular icosahedron. The element distribution Y/Mg on the β positions corresponds to the Ho/Mg distribution (RE_8 cubes). The large temperature factor U_{eq} of Y3 is also mirrored in the same trend for U_{eq}(Ho3) in [16]. Regarding the RE partial structure in fci-Mg–Zn–RE, here is a limit of the 2/1 approximant local structure model and points to a more complicated cluster connecting scheme in the 'true' quasicrystal structure. α^2 and α^3 atoms practically coincide in both fci phases. A difference is observed for the γ atoms: whereas in fci-Ho–Mg–Zn the Zn5 position tends to be occupied by Mg, in the fci-Mg–Y–Zn homologue Mg5 had to be replaced by Zn21. CN 14 allows for both elements at the γ position, whereas it is completely occupied by Zn in the zinc rich compound si-$Ho_{11}Mg_{15}Zn_{74}$ [15]. For the glue atoms, coincidence is found for δ^X (Mg1 and Mg4) and δ^Y (Y5 substitutes for Ho5) positions. A difference is visible at the coordination of the δ^Z position (Zn20): in fci-Ho–Mg–Zn it results in CN 13—on the other hand in fci-Mg–Y–Zn the short distance d(Zn20–Zn20) raises the question of whether there is a split position (resulting in CN 12) or whether there exists a CCT rectangular Z face in the real quasicrystal at all.

4. Conclusion

This structural investigation based on synchrotron powder diffraction data and PDF analysis ($Q_{max} = 30$ Å^{-1}) of fci-Mg–Y–Zn compares to the earlier in-house result for fci-Ho–Mg–Zn ($Q_{max} = 13.5$ Å^{-1}, [16]) quite nicely: PDF refinements for fci-$Mg_{25}Y_{11}Zn_{64}$ ($R = 13.7\%$) confirm the local cluster architecture. Both fci phases show basically the same topological features and element distribution; Y substitutes for Ho in the respective partial RE (RE = Y, Ho) structures. A generic feature is the RE_8 cube (edge length 5.4 Å) inscribed in the second shell of the Bergman cluster. Minor differences in between fci-Mg–Y–Zn and fci-Ho–Mg–Zn point to the limit of the local model: the 'true' cluster connection scheme in the quasicrystal is more complicated; see also [14, 32].

To resolve this problem, large models which contain the RE partial structure only ($\sim$10% of all atoms in the alloy) should be accessible using difference PDFs $\Delta G(r)_{RE} = G(r)_{fci-Ho-Mg-Zn} - G(r)_{fci-Mg-Y-Zn}$ since the substitution of Y by Ho is seen to be isomorphic. This will be the subject of a future publication.

Nevertheless, the refined model that is presented here will be found locally in the icosahedral quasicrystal structure of fci-Mg–Zn–RE alloys. Fci-Zn–Y–Mg can be seen as the representative structure type for the other rare earth analogues fci-Mg–Zn–RE (RE = Dy, Er, Gd, Ho, Tb) reported in the literature.

Acknowledgments

SJB would like to acknowledge help from Didier Wermeille and Doug Robinson for help in collecting data. Work in the Billinge group was supported by Department of Energy (DOE) grant DE-FG02-97ER45651. Data were collected at the 6IDD beamline in the Midwest Universities Collaborative Access Team (MUCAT) sector at the Advanced Photon Source (APS). Use of the APS is supported by the US DOE, Office of Science, Office of Basic Energy Sciences, under contract No W-31-109-Eng-38. The MUCAT sector at the APS is supported by the US DOE, Office of Science, Office of Basic Energy Sciences, through the Ames Laboratory under contract No W-7405-Eng-82.

References

[1] Shechtman D, Blech I, Gratias D and Cahn J W 1984 *Phys. Rev. Lett.* **53** 1951
[2] Steurer W 2004 *Z. Kristallogr.* **219** 391

[3] Luo Z, Zhang S, Tang Y and Zhao D 1993 *Scr. Metall. Mater.* **28** 1513
[4] Tsai A P, Niikura A, Inoue A, Masumoto T, Nishita Y, Tsuda K and Tanaka M 1994 *Phil. Mag. Lett.* **70** 169
[5] Langsdorf A and Assmus W 1998 *J. Cryst. Growth* **192** 152
[6] Fischer I R, Islam Z, Panchula A F, Cheon K O, Kramer M J, Canfield P C and Goldman A I 1998 *Phil. Mag.* B **77** 1601
[7] Estermann M A, Haibach T, Steurer W, Langsdorf A and Assmus W 2000 *Mater. Sci. Eng.* **294–296** 237
[8] Sterzel R, Gross C, Kounis A, Miehe G, Fuess G, Reutzel S, Holland-Moritz D and Assmus W 2002 *Phil. Mag. Lett.* **82** 443
[9] Uhrig E, Brühne S, Sterzel R, Schröpfer L and Assmus W 2003 *Phil. Mag. Lett.* **83** 265
[10] Uhrig E, Brühne S, Assmus W, Grüner D and Kreiner G 2004 *J. Cryst. Growth* at press
[11] Takakura H, Shiono M, Sato T J, Yamamoto A and Tsai A P 2001 *Phys. Rev. Lett.* **86** 236
[12] Kramer M J, Hong S T, Canfield P C, Fischer I R, Corbett J D, Zhu Y and Goldman A I 2002 *J. Alloys Compounds* **342** 82
[13] Ishimasa T, Oyamada K, Arichika Y, Nishibori E, Takata M, Sakata M and Kato K 2003 *J. Non-Cryst. Solids* **334/335** 167
[14] Hong S T and Corbett J D 2003 *Proc. MRS Fall Meeting* p LL7.5
[15] Brühne S, Uhrig E, Gross C and Assmus W 2003 *Cryst. Res. Technol.* **38** 1023
[16] Brühne S, Sterzel R, Uhrig E, Gross C and Assmus W 2004 *Z. Kristallogr.* **219** 245
[17] Billinge S J L and Egami T 2003 *Underneath the Bragg Peaks: Structural Analysis of Complex Materials* (Oxford: Pergamon/Elsevier)
[18] Hahn Th (ed) 1992 *International Tables for Crystallography* vol A (Dordrecht: Kluver–Academic)
[19] Elser V 1985 *Phys. Rev.* B **32** 4892
[20] Billinge S J L and Kanatzidis M G 2004 *Chem. Commun.* 749
[21] Chupas P J, Qiu X, Hanson J C, Lee P L, Grey C P and Billinge S J L 2003 *J. Appl. Crystallogr.* **36** 1342
[22] Hammersley A P, Svenson S O, Hanfland M and Hauserman D 1996 *High Pressure Res.* **14** 235
[23] Qiu X, Thompson J W and Billinge S J L 2004 *J. Appl. Crystallogr.* **37** 678
[24] Proffen T and Billinge S J L 1999 *J. Appl. Crystallogr.* **32** 572
[25] Brandenburg K 1996 *DIAMOND, Informationssystem für Kristallstrukturen* version 2.1c, Universität Bonn
[26] Frank F C and Kasper J S 1958 *Acta Crystallogr.* **11** 184
[27] Shoemaker D P and Shoemaker C B 1986 *Acta Crystallogr.* B **42** 3
[28] Pearson W B 1972 *The Crystal Chemistry and Physics of Metals and Alloys* (New York: Wiley) p 151
[29] Henley C L 1991 *Phys. Rev.* B **43** 993
[30] Kreiner G 2002 *J. Alloys Compounds* **338** 261
[31] Charrier B, Hazemann J L and Schmitt D 1998 *J. Alloys Compounds* **281** 117
[32] Brühne S, Uhrig E, Gross C, Sterzel R, Kreiner G and Assmus W 2004 *Z. Kristallogr.* **21** (Suppl.) 202
[33] Danzer L 2003 private communication